Twelfth Australasian Fluid Mechanics Conference
The University of Sydney, Australia 1995

LDV Measurements in a Swirling Vortex Flow Around a Sphere

Panchapakesan, N.R., Mattner, T., Chong, M.S. and Joubert, P.N.
Department of Mechanical and Manufacturing Engineering
The University of Melbourne
Parkville, Victoria, 3052
AUSTRALIA

ABSTRACT

The motivation for the present study is a desire to further our understanding of the mechanisms by which a material particle is lifted from the bed or floor by the fluid in a turbulent flow. It has been postulated that this might be due to the interaction of vortical structures in the wall boundary layer with the particle rather than by a flow drag mechanism. In order to evaluate this hypothesis a series of experiments involving typical vortical flows and their interaction with a sphere have been designed. This paper reports velocity measurements taken with an LDV system in a swirling flow set up in a cylinder with and without a sphere in the middle.

INTRODUCTION

The physical mechanism by which material particles that are reposing on a surface are entrained into a turbulent fluid flow has not yet been fully clarified. Joubert and Wang (1987) postulated that the particles are lifted from the surface by the action of vortices rather than by a flow drag mechanism. The particle was idealized to be a sphere and the flow around a sphere in different vortical flow configurations was studied.

Joubert and Wang (1987) looked at the flow around spheres of different sizes (15, 30 & 40 mm) in a flow that approximated a Rankine vortex. The vortex was produced in a vertical cylinder of diameter 171 mm and the sphere was positioned in the middle of the cylinder with the help of a sting. Static pressure distributions on the surface of the sphere were measured. They found that, for the strength of the swirl of their experiment, the flow on the upstream surface of the sphere separated while the downstream flow remained attached. They also found that the pressure distribution on the sphere was consistently dependent on the orientation of the sting supporting the sphere (upstream or downstream). Integration of the pressure distribution indicated a net drag force on the sphere which was an order of magnitude larger than for a sphere in an axial flow. A strong restoring force was also exerted on the sphere when it was offset from the axis of the cylinder.

Joubert and Wang (1989) studied the flow around a sphere in a different apparatus that produced a tornado type of vortex. A rotating water tank of 630 mm diameter with a central suction tube was used. The sphere (15 mm dia.) was resting in a bed of spheres of the same diameter. Laser Doppler velocity measurements as well as static pressure measurements were obtained. Lower pressures on the top and relatively high pressures on the bottom gave rise to a net lifting force on the sphere. The flow was found to be attached to the sphere on both sides unlike the earlier experiment. The lifting force was found to decrease as the sphere was moved away from the center of the vortex. When the sphere was raised above the bed, it was found that the lift force increased initially and then asymptoted to a constant value.

Joubert and Wang (1990) extended the measurements of their 1987 work by performing velocity measurements in a similar set-up with a laser Doppler velocimeter. A perspex disk was placed just above the free surface to smooth the entry of the axial flow at the top. In the first instance the sphere was supported by stings both on the upstream side and the downstream side. The interaction of the wake from the sting and the vortex core upstream of the sphere was found to produce higher turbulence levels and larger vortex cores. It was also found that the flow did not separate on the upstream hemisphere as was observed in the earlier investigation. The separated flow on the upstream hemisphere reappeared when the upstream sting was removed. This study confirmed the net drag force on the sphere measured earlier.

Joubert and Wang have not, however, presented

measurements in the absence of an upstream sting. Hence, no quantitative confirmation of upstream separation has yet been made. Furthermore, the basic confined vortex flow was not examined in any detail, particularly with regard to axial variations. Therefore, the aims of this investigation are to examine the basic confined vortex flow and to determine how this flow is altered by the introduction of a sphere.

EXPERIMENTAL SET-UP & MEASUREMENT PROCEDURE

The experimental set-up used for the present investigation is the same as that used by Joubert and Wang (1990) save for some minor modifications indicated below. A schematic sketch of the experimental set-up is shown in Figure 1. Tangential and axial jets provided the water flow to the constant head settling chamber. The relative mass flow through these jets determine the intensity of the swirling motion. The diameter of the inlet manifold supplying water to the tangential jets was increased from 15 mm used by Joubert and Wang (1990) to 100 mm to reduce losses and hence minimize head variations between the tangential jets. The swirling water then flowed through the contraction into the test section and discharged through an annular region to the atmosphere. The annular region was formed by the introduction of the sting supporting the sphere through the discharge hole. An enclosure of square section encased the cylindrical test-section and was filled with stagnant water to minimize optical distortion for LDV measurements.

A sphere of diameter 15 mm was supported on a thin cylindrical rod of diameter 2 mm and length 70 mm mounted on top of a sting of nominal diameter 8 mm. The sting passed through a hole of 14 mm diameter in the bottom plate. This left an annular passage of width 3 mm around the sting as the discharge area for the water. No sting was used upstream of the sphere. The velocity measurements were made with a TSI 9100-7 two component LDV system with TSI IFA 550 counter processors. The Flow Information Display (FIND) software of TSI was used to process the data. This system enabled simultaneous measurements of two velocity components. A total of 5120 samples taken at 0.04 s intervals were used to calculate the mean velocities and average turbulence intensities.

Two component velocity measurements were made along radii perpendicular to one of the flat sides of the square enclosure. In what follows, negative z values denote locations upstream of the sphere (above) and positive z values denote locations downstream of the sphere (below) in millimetres. These measurements were made at axial locations corresponding to $z = \{-100, -50, 0, 50\}$ for the case with no sphere and $z = \{-100, -80, -60, -40, -20, -10\}$ for the case with sphere at $z = 0$.

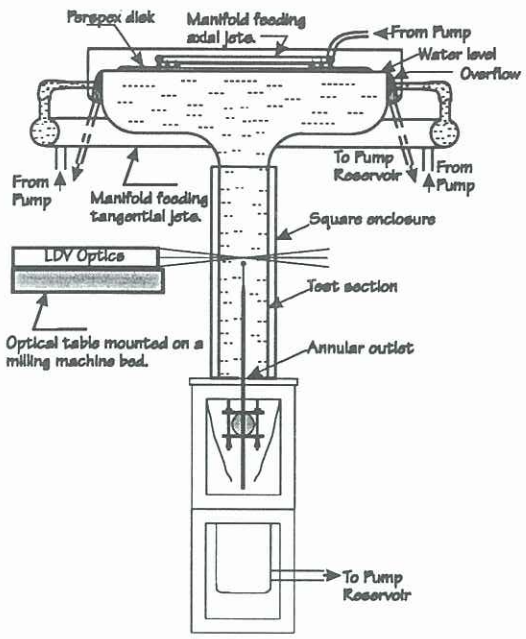

Figure 1: Schematic diagram of the Experimental Set-up

RESULTS

Velocity profiles are presented for one swirl intensity and flow rate. The volume flow rate was approximately 28 L/min. The Reynolds number, based on the average axial velocity determined from the flow rate and the diameter of the cylinder, was 2600. The tangential and axial velocity distributions of the base vortex flow (i.e. without the sphere but with a dummy sting) at various axial locations are shown in Fig. 2 and Fig. 3. Clearly, there is very little variation with distance in the nature of the flow.

The profiles in Fig. 2. resemble the tangential velocity distribution of a Burgers vortex. Escudier

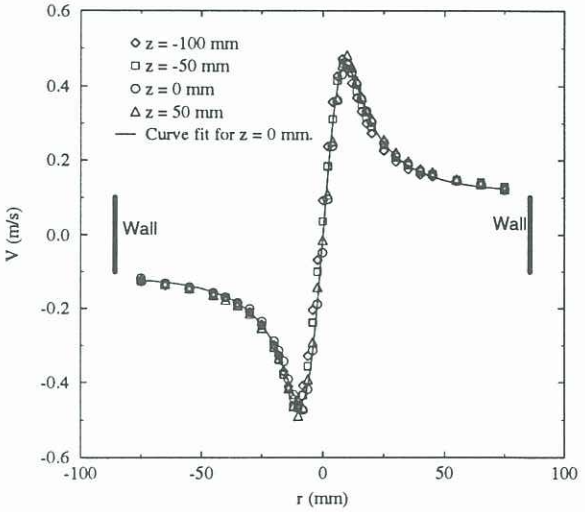

Figure 2: Tangential velocity distribution.

et al. (1982) modified this distribution by adding an additional term that represented the vorticity outside the core:

$$V = (\Gamma_c/2\pi r)(1 - e^{-r^2/\delta^2}) + \frac{1}{2}\omega r$$

where Γ_c represents the circulation around the core and that δ is a length scale corresponding to the radius of the viscous core. Figure 2 also shows an example of a curve fit using the above formula with an additional parameter r' to account for the vortex not being central in the tube or errors in establishing datums. This fit is shown for the case of z = 0. This formulation appears to provide a satisfactory representation of the present measurements.

The axial velocity variations shown in Fig. 3. display two features. The double peak seen near the centre seems to be due to the interaction of the vortex with a bluff body, in this case the dummy sting rather than due to unsteady meandering of the vortex core. Joubert and Wang (1990) do not observe this feature in their results when they used a very short sting placed at the bottom. The other feature is the presence of an annular region of reversed axial flow. Note that a positive velocity is in the mean flow direction ie. down the tube. Flow reversals are a common feature of swirling flows. Three distinct axial flow

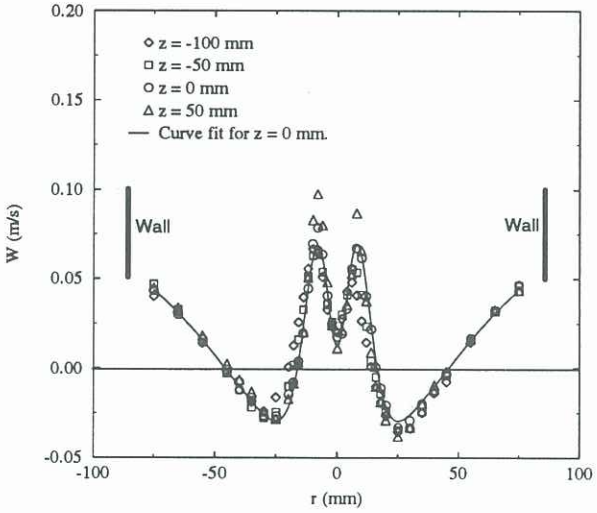

Figure 3: Axial velocity distribution.

regimes have been identified by Nuttal (1953) and, later, by Binnie (1957) using flow visualisation. These are: a) forward flow over the entire cross-section but with a reduced velocity in the centre, b) reversed flow at the centre and forward flow in the outer regions, c) forward flow at the centre and near the walls, but reversed in a narrow region between the axis and the walls. Both these works indicate that regime c) is associated with high rates of swirl. The velocity profile of the present experiments is in this regime. Pressure gradients set up by the swirling flow and interaction of the main flow with the boundary layers have been given as explanations for this observed reverse axial flow.

In Fig. 3. we also show an empirical curve fit of the form:

$$W = W_0 + W_1 e^{-\frac{r^2}{\delta_1^2}} + W_2 e^{-\frac{r^2}{\delta_2^2}} + W_3 e^{-\frac{r^2}{\delta_3^2}}$$

for the axial velocity data for z = 0. (Here also an r' has been included but not shown for brevity). The values of the three δ 's that come out of the curve fit seem to correspond roughly to the tube radius, the vortex core radius and the sting or outlet radius.

In Figures 4 and 5 we compare measurements made with and without the sphere. We have selected the data sets for z = 0 (without sphere) and z = -10 (with sphere). Although comparison at different axial locations is not desirable, as seen in Figures 2 and 3, the nature of the base flow does not change over a large range. Due to difficulties encountered in obtaining satisfactory laser doppler measurements close to surfaces, the results were limited to the region upstream of the sphere. The tangential velocity profile is similar in form to that without the sphere with no significant differences.

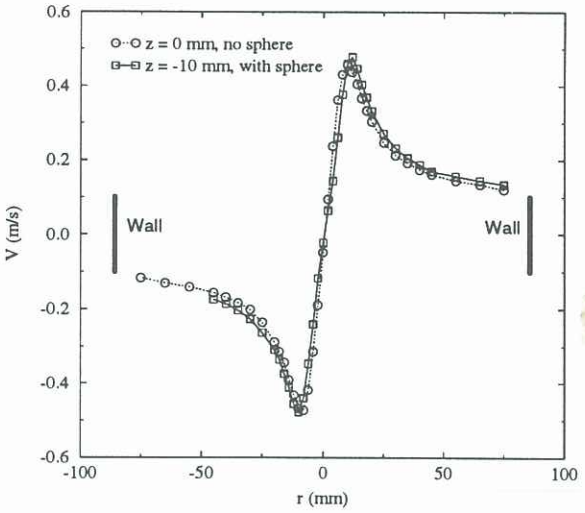

Figure 4: Tangential velocity distribution with sphere.

The axial mean velocity distribution shown in Figure 5 indicates that the presence of the sphere results in flow reversal near the center. This is also seen at z = -20. This is consistent with the flow visualisations reported by Joubert and Wang (1987). This flow reversal or upstream separation was not measured in the LDV measurements performed by Joubert and Wang (1990) when the sphere was supported by both upstream and downstream stings.

Figures 6 and 7 show typical root mean square velocities for the tangential and axial directions. In both cases there is a significant increase in the measured turbulence near the centre of the tube. Observations of the pressure induced dip at the free surface and dye flow visualisations of the core indicate

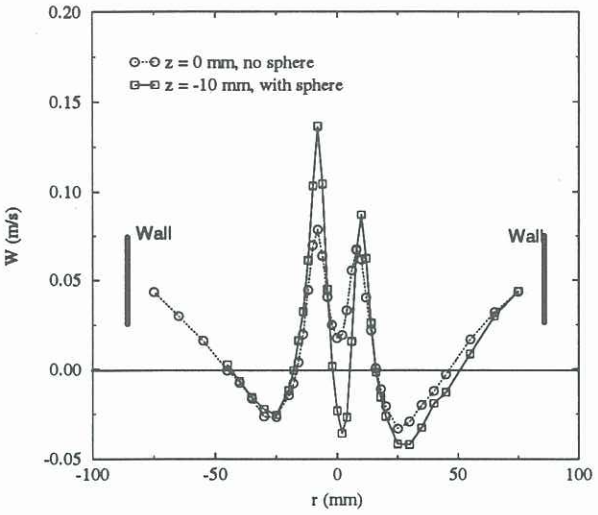

Figure 5: Axial velocity distribution with sphere.

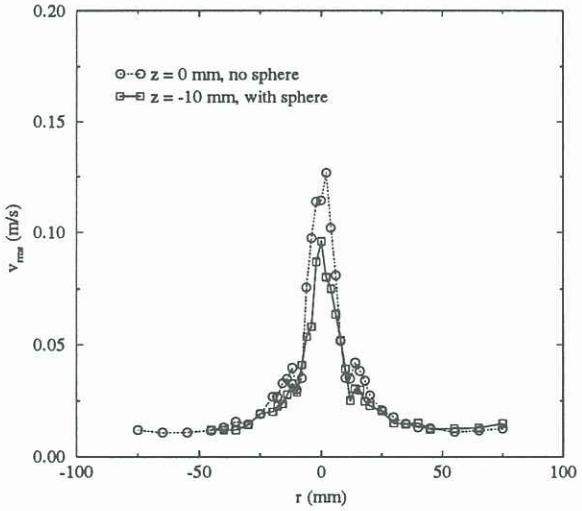

Figure 6: Rms value of tangential velocity fluctuations.

that, despite the improvements made to the swirling flow entry, the core position is unsteady. If the radial distributions of velocity fluctuated in position, then large velocity gradients would be expected to produce large variations in velocity at a fixed point. Inspection of the plots shows that the peaks in the root mean square velocity correspond to maximum velocity gradients. Auto-correlations of the fluctuating velocity also show a periodicity near the center of the sphere hence it appears likely that they are caused by the unsteadiness or 'wobble' observed in the position of the core.

CONCLUSIONS

1. The existence and formation of reversed flows in the basic flow needs to be properly understood before we examine the additional complication created by adding a sphere.

2. The existence of upstream separation or flow reversal ahead of the sphere has been quantitatively confirmed in the present apparatus. (Joubert and

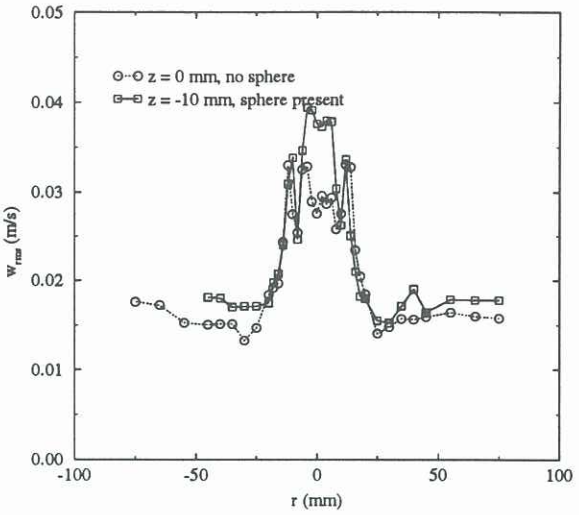

Figure 7: Rms value of axial velocity fluctuations.

Wang (1990) found that this feature is destroyed by the addition of an upstream sting).

3. The tangential velocity profile is well described by the modified Burgers distribution.

4. Axial velocities appear to be well represented by:

$$W = W_0 + W_1 e^{-\frac{r^2}{\delta_1^2}} + W_2 e^{-\frac{r^2}{\delta_2^2}} + W_3 e^{-\frac{r^2}{\delta_3^2}}$$

. 5. Peaks in rms velocity may be attributed to vortex wobble or unsteadiness.

REFERENCES

1. Binnie, A.M., (1957), "Experiments on the Slow Swirling Flow of a Viscous Liquid Through a Tube," *Quart. J. Mech. and Applied Math.* v. 3, p. 276.

2. Escudier, M.P., Bornstein, J. and Maxworthy, T., (1982), "The Dynamics of Confined Vortices," *Proc. R. Soc. Lond.* v. A382, p 335.

3. Joubert, P.N. and Wang, M.H., (1987), "Drag on a Sphere in Swirling Flow", *Sixth Symposium, Turbulent Shear Flows, Toulouse, France.*

4. Joubert, P.N. and Wang, M.H., (1989), "Lift on a Grounded Sphere under a Tornado Vortex", *Seventh Symposium, Turbulent Shear Flows, Stanford, California, U.S.A.*

5. Joubert, P.N. and Wang, M.H., (1990), "LDA Measurements of the Flow Field About an Isolated Sphere in Swirling Flow", *Sixth International Symposium on Applications of Laser Techniques to Fluid Mechanics - July 1990.*

6. Nuttal, J.B., (1953), "Axial Flow in a Vortex", *Nature*, v. 172, p. 582.